

## MIT Open Access Articles

*High Charge Mobility in a Tetrathiafulvalene-Based Microporous Metal–Organic Framework*

The MIT Faculty has made this article openly available. *Please share* how this access benefits you. Your story matters.

**Citation:** Narayan, Tarun C., Tomoyo Miyakai, Shu Seki, and Mircea Dincă 2012 High Charge Mobility in a Tetrathiafulvalene-Based Microporous Metal–Organic Framework. *Journal of the American Chemical Society* 134(31): 12932–12935.

**As Published:** <http://dx.doi.org/10.1021/ja3059827>

**Publisher:** American Chemical Society

**Persistent URL:** <http://hdl.handle.net/1721.1/79703>

**Version:** Author's final manuscript: final author's manuscript post peer review, without publisher's formatting or copy editing

**Terms of Use:** Article is made available in accordance with the publisher's policy and may be subject to US copyright law. Please refer to the publisher's site for terms of use.



# High Charge Mobility in a Tetrathiafulvalene-Based Microporous Metal-Organic Framework

Tarun C. Narayan,<sup>†</sup> Tomoyo Miyakai,<sup>‡</sup> Shu Seki,<sup>‡</sup> and Mircea Dincă<sup>†\*</sup>

<sup>†</sup>Department of Chemistry, Massachusetts Institute of Technology, 77 Massachusetts Avenue, Cambridge, MA, 02139, USA

<sup>‡</sup>Department of Applied Chemistry, Graduate School of Engineering, Osaka University, Suita, Osaka 565-0871, Japan

Supporting Information Placeholder

The tetratopic ligand tetrathiafulvalene-tetrabenzoate ( $H_4$ TTFTB) is used to synthesize  $Zn_2$ (TTFTB), a new metal-organic framework that contains columnar stacks of tetrathiafulvalene and benzoate-lined infinite one-dimensional channels. The new MOF remains porous upon desolvation and exhibits charge mobility commensurate with some of the best organic semiconductors, confirmed by flash-photolysis-time-resolved microwave conductivity measurements.  $Zn_2$ (TTFTB) represents the first example of a permanently porous MOF with high charge mobility and may inspire further exploration of the electronic properties of these materials.

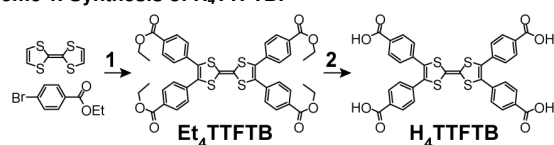
High surface area conductive materials are poised to transform the energy landscape in the near future. Microporous conductive ceramics and activated carbons have become the norm in high temperature fuel cells and supercapacitors,<sup>1-3</sup> while porous chalcogenide semiconductors and conductive polymers are attractive targets for applications in electrocatalysis, separation, and sensing technologies.<sup>4-6</sup> One class of materials with a great impact potential in this area is metal-organic frameworks (MOFs). These have high intrinsic porosity that has led to applications in gas separation and storage among others,<sup>7-9</sup> but typically exhibit very low electronic conductivity, which drastically impairs their utility as high surface area conductors. The low conductivity of porous MOFs is not surprising: they are usually made from hard metal ions connected by redox-inactive organic ligands; this combination does not provide a good conjugation pathway for charge transport. As such, one of the most challenging and potentially rewarding endeavors in this rapidly expanding field is to synthesize porous frameworks that show good charge mobility and conductivity.<sup>10</sup>

One means to address this challenge is to use softer, sulfur-based bridging ligands that form more covalent interactions with the metal ions. For instance, di- and tetra-thiobenzenes were known to form conductive non-porous coordination polymers<sup>11-14</sup> and served as inspiration for the only two examples of permanently porous and electronically conductive MOFs.<sup>15,16</sup> An alternative to engineering through-bond charge delocalization<sup>17,18</sup> is to employ  $\pi$ -stacks of electroactive molecules as the charge transport pathways. Most famously exemplified by charge transfer salts such as tetrathiafulvalene-tetracyanoquinodimethane (TTF-TCNQ),<sup>19,20</sup>  $\pi$ -stacked molecular crystals can exhibit metallic conductivity and even superconductivity.<sup>21,22</sup> They inspired the development of electroactive covalent-organic frameworks (COFs), wherein

stacked layers of flat  $\pi$  molecules such as porphyrins, phthalocyanines, or triphenylenes define microporous structures with high photoconductivity and/or charge mobility.<sup>23-28</sup>

We sought to apply a similar strategy to design MOFs with high charge mobility. In doing so, we focused on TTF as a building block, hoping that its high propensity to  $\pi$ -stack would balance well with the stronger driving force of the metal-ligand bond formation, thereby enforcing the construction of a material that exhibits both porosity and a pathway for efficient charge transport. Although there have been attempts to control the supramolecular structure of TTF-based materials while retaining conductivity, such as through  $N\cdots I n \rightarrow \sigma^*$  interactions,<sup>29</sup> coordination to metal ions through thioalkyl groups,<sup>30</sup> and carboxylates directly appended onto the TTF core,<sup>31-33</sup> none have resulted in permanently porous materials. Herein we show that a TTF-based ligand containing benzoate spacers generates a zinc-based MOF that exhibits both columnar stacks of TTF and permanent pores lined by benzoate linkers. The material displays charge mobility of a magnitude that matches some of the best conductive organic polymers, as determined by flash photolysis-time resolved microwave conductivity (FP-TRMC). To our knowledge, this is the first measurement of the intrinsic charge mobility in a permanently porous MOF, and sets a standard that should encourage a sustained research effort in this area.

**Scheme 1. Synthesis of  $H_4$ TTFTB.**



1:  $Cs_2CO_3$ ,  $Pd(OAc)_2$ ,  $(HP^tBu_3)(BF_4)$  in THF, 18 h reflux

2: KOH in  $CH_3OH$ ,  $H_2O$ , THF, 12 h reflux

The ligand tetrathiafulvalene-tetrabenzoate ( $H_4$ TTFTB) was synthesized in two steps through a palladium-catalyzed cross coupling between TTF and ethyl-4-bromobenzoate<sup>34</sup> followed by saponification<sup>35</sup> (see Scheme 1). Treatment of a solution of  $H_4$ TTFTB in 3:1 DMF/EtOH with a solution of  $Zn(NO_3)_2 \cdot xH_2O$  in 1:1 EtOH/ $H_2O$  followed by heating at 75°C for two days afforded the  $[Zn_2TTFTB(H_2O)_2] \cdot H_2O \cdot 2DMF$  (**1**) as dark red needles.

X-ray diffraction analysis of a single crystal of **1** revealed a structure comprised of infinite helical chains of corner-sharing pseudo-octahedra joined together by helical stacks of TTFTB<sup>†</sup> linkers (see Figure 1). Compound **1** crystallizes in the space group  $P6_5$  with a racemic twinning domain. The  $6_5$  screw axis

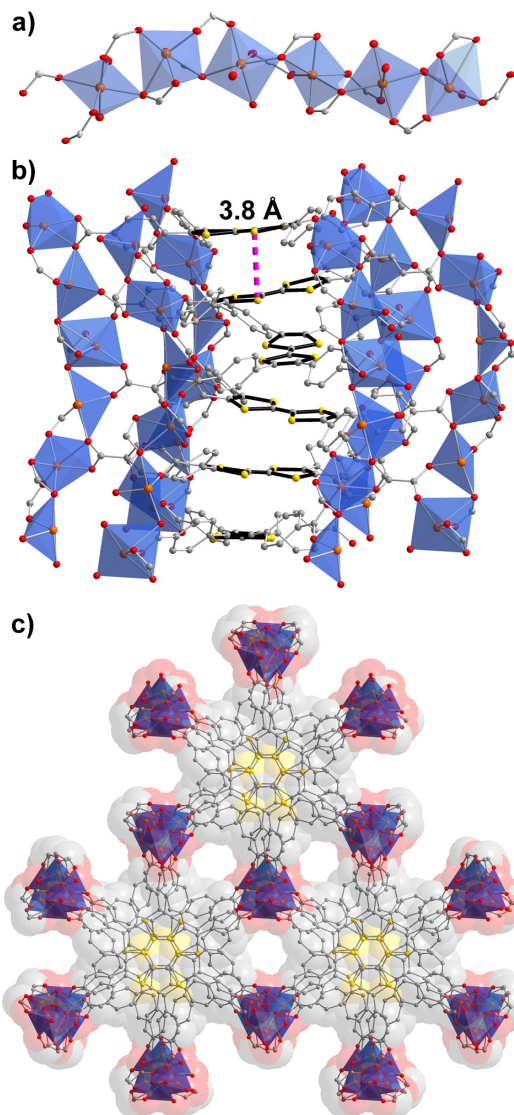


**Figure 1.** Portions of the crystal structure of **1**: (a) the infinite helical Zn-carboxylate chains, (b) a side view of a helical TTF stack with a depiction of the shortest intermolecular S...S contact, and (c) a view of the benzoate-lined infinite pores down the *c* axis. Orange, yellow, red, and grey spheres represent Zn, S, O, and C atoms, respectively. H atoms and water molecules in (b) were omitted for clarity.

bisects the central ethylene unit of the TTF core of  $\text{TTFTB}^{4-}$ , such that adjacent TTF units are rotated by  $60^\circ$  relative to one another and translated by  $3.47 \text{ \AA}$  in the *c* direction. The two dithiole rings in each TTF core are slightly twisted around the central ethylene bond to give a dihedral angle of  $2.32^\circ$ . The phenyl rings also exhibit a significant torsion with respect to the TTF core, defining dihedral angles ranging from  $40^\circ$  to  $52^\circ$  with the latter. Together with the helical metal-carboxylate chains that run roughly perpendicular to the TTF cores, the benzoate groups delineate cylindrical pores with a van der Waals diameter of  $\sim 5 \text{ \AA}$ . Finally, the infinite metal-carboxylate chains are built from two crystallographically independent Zn atoms, each of which exhibits a pseudo-octahedral coordination sphere of six oxygen atoms pertaining to carboxylates in one case and four carboxylates and two *cis*-oriented water molecules in the other case. Importantly, alt-

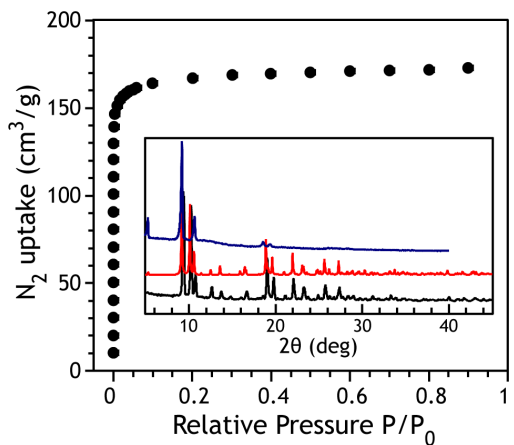


**Figure 2.** Isotherm for the adsorption of  $\text{N}_2$  in **1** at 77 K. The inset shows the powder X-ray diffraction patterns of as-synthesized **1** (black), simulated **1** (red), and desolvated **1** (blue).

hough the TTF cores are not perpendicular to the screw axis, one relatively close intermolecular S...S contact of  $3.803(2) \text{ \AA}$  is found between neighboring TTF moieties in **1**. This value is similar to the range of intermolecular S...S distances found in TTF-TCNQ and other conductive charge-transfer salts,<sup>36-39</sup> and it encouraged us to further investigate the potential for charge mobility in **1**.

Thermogravimetric analysis (TGA) of **1**, shown in Figure S1, exhibits a sharp mass loss of 28.3 % between  $100^\circ\text{C}$  and  $140^\circ\text{C}$ , which agrees well with the 28.2 % mass loss expected for the elimination of 3.5 guest DMF molecules and coordinated water. Importantly, TGA suggested that **1** exhibits a large plateau of thermal stability above  $180^\circ\text{C}$  until the final decomposition upwards of  $400^\circ\text{C}$ . Evacuation of **1** was accordingly performed by heating as-synthesized material at  $200^\circ\text{C}$  and 4 mtorr for 12 hours. Its crystallinity and identity were confirmed by powder X-ray diffraction (Figure 2, inset) and elemental analysis, respectively, which indicated that the structure is maintained upon evacuation and exposure to air and that indeed all solvent molecules are removed. Upon desolvation, **1** absorbs  $\sim 170 \text{ cm}^3/\text{g}$  of  $\text{N}_2$  at 77 K and displays a Type I isotherm, confirming its microporous nature (see Figure 2). A BET analysis of the isotherm data revealed a permanently porous structure with an apparent surface area of  $662 \text{ m}^2/\text{g}$  and confirmed **1** as the first crystalline TTF-based material with intrinsic microporosity. Analysis of the  $\text{N}_2$  isotherm data using the Tarazona non-local density functional theory<sup>40</sup> also revealed a narrow pore size distribution centered around  $6 \text{ \AA}$ , in agreement with the pore size expected from a space filling model of **1**.

Interestingly, an EPR spectrum of as-synthesized **1**, shown in Figure S2, displayed a sharp signal at  $g = 2.006$  characteristic of organic-based radicals, and suggested that TTF cores in **1** are at least partially oxidized during the MOF synthesis and that **1** is already partially doped in its as-synthesized form. To confirm that the radical character of **1** is centered on the TTF moieties, the free ligand  $\text{H}_4\text{TTFTB}$  was oxidized with  $\text{I}_2$  in ethanol and the product displayed an EPR signal centered at  $g = 2.006$  as well. Encouraged by the inherent partial doping of **1** and by the relatively short S...S distances between neighboring TTF cores, we sought to investigate the conductive properties of this MOF. Because of the anisotropic structure of **1**, we expected that its bulk conductivity would be greatly affected

not just by grain boundary resistances, but also by the highly randomized orientation of individual grains within a pellet or a film. Low bulk conductivity values defined by an average of the conductivity in all three directions are well documented in charge-transfer salts and other one-dimensional conductors.<sup>41</sup>

To eliminate anisotropy effects in our electrical measurements, we explored the conductivity of as-synthesized **1** using FP-TRMC. This technique allows the measurement of charge mobility on the multi-nanometer length scale, much smaller than the size of an individual grain or crystallite, and is therefore indicative of the intrinsic charge mobility of a given material.<sup>42,43</sup> The technique effectively eliminates almost all of the perturbations resulting from impurities, grain boundaries, electrode contacts and, most importantly, the directionality of charge transport, whose influences are unavoidable in other configurations such as pressed pellets and field-effect transistors (FETs). FP-TRMC measurements were carried out in ambient conditions on films made from **1** and PMMA (40/60 wt%). Samples were pulsed with 355 nm light, and the charge carrier generation efficiency was obtained by a time-of-flight (TOF) transient current integration. The FP-TRMC profiles for **1** and a similar film made from H<sub>4</sub>TTFTB, both shown in Figure 3a, display maximum values of  $\phi\Sigma\mu$  of  $3 \times 10^{-5}$  and  $9 \times 10^{-6}$  cm<sup>2</sup>/V·s, respectively, where  $\phi$  is the photocarrier generation yield and  $\Sigma\mu$  is the sum of the generated charge carrier mobilities for both electrons and holes. The TOF current transients, shown in Figure 3b, give  $\phi$  values of  $4 \times 10^{-3}$  and  $2 \times 10^{-4}$  for H<sub>4</sub>TTFTB and **1**, respectively. Because of the higher value of  $\phi$  in H<sub>4</sub>TTFTB, its current transient response could be verified using transient absorption measurements, an entirely non-contact technique. Transient absorption spectra of H<sub>4</sub>TTFTB dispersed in PMMA matrices and the corresponding kinetic trace observed at 650 nm (1.9 eV) are shown in Figure S10. Notably, this band is red-shifted from that observed for an isolated TTF radical cation (2.17 eV), but blue-shifted relative to that expected for a mixed-valent TTF radical cation dimer (1.69 eV),<sup>44,45</sup> suggesting increased delocalization over neighboring TTF cores in H<sub>4</sub>TTFTB. Most importantly, the  $\phi$  value for H<sub>4</sub>TTFTB obtained by transient absorption measurements,  $2.5 \times 10^{-3}$ , agrees well with that obtained from the TOF measurements and suggests that holes are the major carriers in H<sub>4</sub>TTFTB and, by analogy, in **1**.

Combined, the FP-TRMC and TOF current transient measurements reveal an outstanding intrinsic charge mobility of 0.2 cm<sup>2</sup>/V·s for **1**. This value is two orders of magnitude higher than that found for H<sub>4</sub>TTFTB, and is in line with values found for highly-oriented porphyrin and phthalocyanine-based COFs.<sup>23,24,26-28</sup> Most remarkably, the charge mobility in **1** is higher than those found for common organic conductors such as some polyphenylenevinylenes ( $\mu = 0.01 - 0.1$  cm<sup>2</sup>/V·s)<sup>46</sup> and polythiophenes ( $\mu = 0.015 - 0.075$  cm<sup>2</sup>/V·s)<sup>47</sup> measured by the same technique. We note also that even polythiophenes used in organic photovoltaic devices, such as poly(3-hexylthiophene) and poly(2,5-bis(3-alkylthiophen-2-yl)thieno[3,2-b]thiophene have field-effect (bulk) mobilities of approximately 0.1 and 0.2-0.6 cm<sup>2</sup>/V·s, respectively.<sup>48,49</sup>

It is stimulating to discuss the nature of the charge delocalization in **1**, which displays high charge mobility despite its unusual and less-than-ideal TTF stacking sequence that allows only one relevant intermolecular S···S contact. To test whether a band model is an appropriate description of the electronic structure of **1**, one can apply the energy-time uncertainty prin-

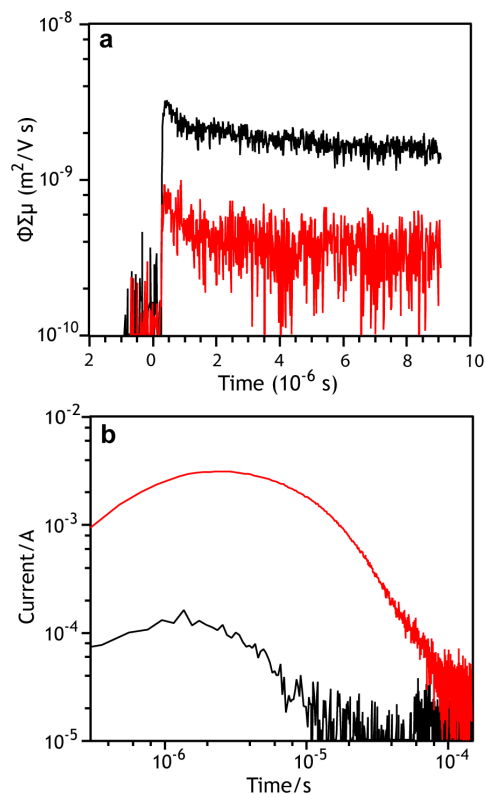


**Figure 3.** (a) Conductivity transients observed by FP-TRMC upon excitation at 355 nm with  $6.5 \times 10^{15}$  cm<sup>-2</sup> photons per pulse for **1** (black trace) and H<sub>4</sub>TTFTB (red trace); (b) photocurrent transients observed for 20-26 μm thick solid films of materials in PMMA matrices sandwiched between Au-semi-transparent and Al electrodes. The transients were observed with a terminate resistance of 10 kΩ under applied bias at  $1.2 - 1.5 \times 10^4$  V/cm.

ciple by assuming a typical electron-lattice scattering time of  $\tau = 10^{-14}$  s and a spacing of 3.81 Å between components. Using these values, the minimum charge mobility necessary for treating a system with a band model is 0.3 cm<sup>2</sup>/V·s.<sup>50</sup> This is only slightly larger than the mobility value found in **1**, suggesting that our system can indeed be described as partially delocalized. This analysis also suggests that if the molecular overlap between neighboring TTF cores can be engineered to either increase the number of S···S contacts or shorten the length of the contacts, MOFs with even higher charge mobility may be accessible.

In summary, we have shown that the use of a benzoate-extended TTF core leads to a permanently porous MOF that shows very high intrinsic charge mobility within the class of organic-based conductors. Many challenges must be overcome before such materials will be implemented in functional electronic devices, not least of which is their processing as oriented thin films for interfacing with electrodes.<sup>51,52</sup> Nevertheless, these results demonstrate that MOFs are amenable to designs that promote good charge transfer among the individual building blocks. We hope that this study will inspire the exploration of the electronic properties of MOFs, which have received comparatively less attention than more traditional applications such as gas storage and separation.

## ASSOCIATED CONTENT

**Supporting Information.** Experimental details, table of X-ray refinement details, TGA trace, EPR spectra, additional graphs from the isotherm data, NMR and transient absorption spectra of

H<sub>4</sub>TTFTB, and an ORTEP representation of a portion of the structure of **1**. This material is available free of charge via the Internet at <http://pubs.acs.org>.

## AUTHOR INFORMATION

### Corresponding Author

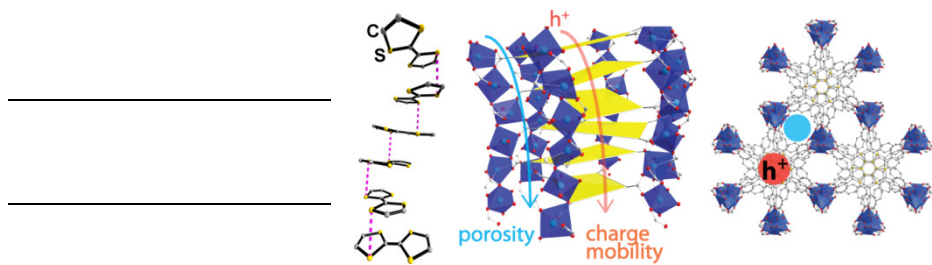
mdinca@mit.edu

### ACKNOWLEDGMENT

This work was supported by the U.S. Department of Energy, Office of Science, Office of Basic Energy Sciences under Award Number DE-SC0006937. Grants from the NSF provided instrument support to the DCIF at MIT (CHE-9808061, DBI-9729592). This work made use of the MRSEC Shared Experimental Facilities at MIT, supported in part by the NSF under award number DMR-0819762. We thank Dr. N. Shustova for assistance with the X-ray data analysis.

### REFERENCES

- (1) Brandon, N. P.; Brett, D. J. *Philos. Trans. A* **2006**, *364*, 147.
- (2) Simon, P.; Gogotsi, Y. *Nature Mater.* **2008**, *7*, 845.
- (3) Kondrat, S.; Pérez, C. R.; Presser, V.; Gogotsi, Y.; Kornyshev, A. A. *Energy Environ. Sci.* **2012**, *5*, 6474.
- (4) Yuhas, B. D.; Smeigh, A. L.; Samuel, A. P. S.; Shim, Y.; Bag, S.; Douvalis, A. P.; Wasielewski, M. R.; Kanatzidis, M. G. *J. Am. Chem. Soc.* **2011**, *133*, 7252.
- (5) Bag, S.; Gaudette, A. F.; Bussell, M. E.; Kanatzidis, M. G. *Nature Chem.* **2009**, *1*, 217-24.
- (6) Zheng, N.; Bu, X.; Feng, P. *Nature* **2003**, *426*, 428.
- (7) Sumida, K.; Rogow, D. L.; Mason, J. A.; McDonald, T. M.; Bloch, E. D.; Herm, Z. R.; Bae, T.-H.; Long, J. R. *Chem. Rev.* **2012**, *112*, 724.
- (8) Li, J.-R.; Sculley, J.; Zhou, H.-C. *Chem. Rev.* **2012**, *112*, 869.
- (9) Férey, G.; Millange, F.; Morcrette, M.; Serre, C.; Doublet, M.-L.; Grenèche, J.-M.; Tarascon, J.-M. *Angew. Chem. Int. Ed.* **2007**, *46*, 3259.
- (10) Givaja, G.; Amo-Ochoa, P.; Gómez-García, C. J.; Zamora, F. *Chem. Soc. Rev.* **2012**, *41*, 115.
- (11) Vogt, T.; Faulmann, C.; Soules, R.; Lecante, P.; Mosset, A.; Castan, P.; Cassoux, P.; Galy, J. J. *J. Am. Chem. Soc.* **1988**, *110*, 1833.
- (12) Jolly, C. A.; Wang, F.; Krichene, S.; Reynolds, J. R.; Cassoux, P.; Faulmann, C. *Synth. Met.* **1989**, *29*, 189.
- (13) Schrauzer, G. N.; Prakash, H. *Inorg. Chem.* **1975**, *14*, 1200.
- (14) Dirk, C. W.; Bousseau, M.; Barrett, P. H.; Moraes, F.; Wudl, F.; Heeger, A. J. *Macromolecules* **1986**, *19*, 266.
- (15) Kobayashi, Y.; Jacobs, B.; Allendorf, M. D.; Long, J. R. *Chem. Mater.* **2010**, *22*, 4120.
- (16) Takaishi, S.; Hosoda, M.; Kajiwara, T.; Miyasaka, H.; Yamashita, M.; Nakanishi, Y.; Kitagawa, Y.; Yamaguchi, K.; Kobayashi, A.; Kitagawa, H. *Inorg. Chem.* **2009**, *48*, 9048.
- (17) Avendano, C.; Zhang, Z.; Ota, A.; Zhao, H.; Dunbar, K. R. *Angew. Chem. Int. Ed.* **2011**, *50*, 6543.
- (18) Ballesteros-Rivas, M.; Ota, A.; Reinheimer, E.; Prosvirin, A.; Valdés-Martínez, J.; Dunbar, K. R. *Angew. Chem. Int. Ed.* **2011**, *50*, 9703.
- (19) Ferraris, J.; Cowan, D. O.; Walatka, V.; Perlstein, J. H. *J. Am. Chem. Soc.* **1973**, *95*, 948.
- (20) Bryce, M. R. *Chem. Soc. Rev.* **1991**, *20*, 355.
- (21) Williams, J. M.; Schultz, A. J.; Geiser, U.; Carlson, K. D.; Kini, A. M.; Wang, H. H.; Kwok, W. K.; Whangbo, M. H.; Schirber, J. E. *Science* **1991**, *252*, 1501.
- (22) Jerome, D.; Mazaud, A.; Ribault, M.; Bechgaard, K. *J. Physique Lett.* **1980**, *41*, 95.
- (23) Feng, X.; Chen, L.; Honsho, Y.; Saengsawang, O.; Liu, L.; Wang, L.; Saeki, A.; Irle, S.; Seki, S.; Dong, Y.; Jiang, D. *Adv. Mater.* **2012**, *24*, 3026.
- (24) Feng, X.; Liu, L.; Honsho, Y.; Saeki, A.; Seki, S.; Irle, S.; Dong, Y.; Nagai, A.; Jiang, D. *Angew. Chem. Int. Ed.* **2012**, *51*, 2618.
- (25) Spittler, E. L.; Dichtel, W. R. *Nature Chem.* **2010**, *2*, 672.
- (26) Wan, S.; Gándara, F.; Asano, A.; Furukawa, H.; Saeki, A.; Dey, S. K.; Liao, L.; Ambrogio, M. W.; Botros, Y. Y.; Duan, X.; Seki, S.; Stoddart, J. F.; Yaghi, O. M. *Chem. Mater.* **2011**, *23*, 4094.
- (27) Wan, S.; Guo, J.; Kim, J.; Ihee, H.; Jiang, D. L. *Angew. Chem. Int. Ed.* **2008**, *47*, 8826.
- (28) Wan, S.; Guo, J.; Kim, J.; Ihee, H.; Jiang, D. *Angew. Chem. Int. Ed.* **2009**, *48*, 5439.
- (29) Imakubo, T.; Maruyama, T.; Kobayashi, K.; Sawa, H. *Chem. Commun.* **1998**, 2021.
- (30) Munakata, M.; Kuroda-Sowa, T.; Maekawa, M.; Hirota, A.; Kitagawa, S. *Inorg. Chem.* **1995**, *34*, 2705.
- (31) Qin, Y.-R.; Zhu, Q.-Y.; Huo, L.-B.; Shi, Z.; Bian, G.-Q.; Dai, J. *Inorg. Chem.* **2010**, *49*, 7372.
- (32) Nguyen, T. L. A.; Devic, T.; Mialane, P.; Rivière, E.; Sonnauer, A.; Stock, N.; Demir-Cakan, R.; Morcrette, M.; Livage, C.; Marrot, J.; Tarascon, J.-M.; Férey, G. *Inorg. Chem.* **2010**, *49*, 10710.
- (33) Nguyen, T. L. A.; Demir-Cakan, R.; Devic, T.; Morcrette, M.; Ahnfeldt, T.; Auban-Senzier, P.; Stock, N.; Goncalves, A.-M.; Filinchuk, Y.; Tarascon, J.-M.; Férey, G. *Inorg. Chem.* **2010**, *49*, 7135.
- (34) Mitamura, Y.; Yorimitsu, H.; Oshima, K.; Osuka, A. *Chem. Sci.* **2011**, *2*, 2017.
- (35) Li, J.-R.; Zhou, H.-C. *Angew. Chem. Int. Ed.* **2009**, *48*, 8465.
- (36) Aumüller, A.; Erk, P.; Hünig, S.; Schiitz, J. U. V.; Werner, H.-P.; Wole, H. C.; Klebe, G. *Chem. Ber.* **1991**, *124*, 1445.
- (37) Williams, R.; Lowe Ma, C.; Samson, S.; Khanna, S. K.; Somoano, R. B. *J. Chem. Phys.* **1980**, *72*, 3781.
- (38) Blessing, R. H.; Coppens, P. *Solid State Commun.* **1974**, *15*, 215.
- (39) Mori, T.; Inokuchi, H. *Bull. Chem. Soc. Japan* **1992**, *65*, 1460.
- (40) Webb, P. A.; Orr, C. *Analytical Methods in Fine Particle Technology*; Micromeritics Instr. Corp.: Norcross, GA, 1997.
- (41) Wheland, R. C.; Gillson, J. L. *J. Am. Chem. Soc.* **1976**, *98*, 3916.
- (42) Saeki, A.; Seki, S.; Koizumi, Y.; Tagawa, S. *J. Photoch. Photobiol. A* **2007**, *186*, 158.
- (43) Saeki, A.; Koizumi, Y.; Aida, T.; Seki, S. *Acc. Chem. Res.* **2012**, ASAP Articles, DOI: 10.1021/ar200283b.
- (44) Yoshizawa, M.; Kumazawa, K.; Fujita, M. *J. Am. Chem. Soc.* **2005**, *127*, 13457.
- (45) Rosokha, S. V.; Kochi, J. K. *J. Am. Chem. Soc.* **2007**, *129*, 828.
- (46) Krebs, F. C.; Jørgensen, M. *Macromolecules* **2003**, *36*, 4374.
- (47) Saeki, A.; Seki, S.; Koizumi, Y.; Sunagawa, T.; Ushida, K.; Tagawa, S. *J. Phys. Chem. B* **2005**, *109*, 10015.
- (48) Sirringhaus, H.; Brown, P. J.; Friend, R. H.; Nielsen, M. M.; Bechgaard, K.; Langeveld-Voss, B. M. W.; Spiering, A. J. H.; Janssen, R. A. J.; Meijer, E. W.; Herwig, P.; de Leeuw, D. M. *Nature* **1999**, *401*, 685.
- (49) McCulloch, I.; Heeney, M.; Bailey, C.; Genevicius, K.; Macdonald, I.; Shkunov, M.; Sparrowe, D.; Tierney, S.; Wagner, R.; Zhang, W.; Chabinyc, M. L.; Kline, R. J.; McGehee, M. D.; Toney, M. F. *Nature Mater.* **2006**, *5*, 328.
- (50) Bright, A.; Chaikin, P.; McGhie, A. *Phys. Rev. B* **1974**, *10*, 3560.
- (51) Li, M.; Dincă, M. *J. Am. Chem. Soc.* **2011**, *133*, 12926.
- (52) Bétard, A.; Fischer, R. A. *Chem. Rev.* **2012**, *112*, 1055.



TOC Graphic.